

Evaluation of the Deceleration Rate for the Operating Speed-Profile Model

Ph.D. Ing. Paolo Perco
Department of Civil Engineering, University of Trieste

Ing. Alberto Robba
Department of Civil Engineering, University of Trieste

Synopsis

The Italian Standard uses the design speed-profile to check the consistency of the horizontal alignment and to avoid dangerous changes in speed. However, the real speed used by the driver to travel a curve can differ significantly from the design speed of the same curve. Moreover, the speed reached along tangents can also differ from the maximum design speed of the road. Therefore, an operating speed-profile was proposed in order to better represent the real speed used by the driver and, consequently, to check the consistency of the alignment. This profile uses operating speed models to predict the operating speed of the geometric elements (circular curves and long tangents) as a function of their geometric characteristics. However, even though these models enable us to give a good estimation of the real speed along the single elements, there is still little information about how the driver varies the speed between successive elements. Real acceleration and deceleration rates, as well as driver behaviour between curves with different operating speeds separated by short tangents, are only presumed. Therefore, a new research using a light detection and ranging (lidar) gun was set up to improve knowledge of speed variations along the transition sections. The primary object of the research is to establish conclusively deceleration/acceleration rates, and driver speed behaviour approaching/departing from curves. The first step in the research involved the collection of a sample of speed-data to evaluate speed reduction approaching a circular curve. This subject was selected as the first step because, given the nature of curve-related accidents, accurate deceleration rates are more important in the model than acceleration rates. The speed data were collected on 10 sites composed of a curve and preceding tangent. The paper presents the preliminary results of the data analysis. Two different approaches were used to calculate the deceleration rates from the speed data and these approaches led to significantly different rates. The analysis indicates that a deceleration rate of $0,85 \text{ m/s}^2$ can be used in a simplified operating speed-profile, but this value represents only a rough approximation of the real deceleration rates. In fact, the deceleration rate varies along the distance travelled during the speed reduction before the curve. In particular, the data shows that in the final part of the speed reduction the deceleration rate is higher than in the first part. Moreover, the results show that the deceleration rate varies significantly between different curves. These differences could be due to many factors such as the characteristics of the curve, of the upstream alignment, of the overall road environment. The research will continue to investigate these relationships collecting additional data on new sites.

Evaluation of the Deceleration Rate for the Operating Speed-Profile Model

The Italian standard uses the design speed-profile to check the consistency of the horizontal alignment. The procedure used to trace this profile, similar to that used by the Swiss standard, includes numerous hypotheses, some of which are not confirmed by experimental results. The most important of them is that the real speed used by the driver to travel geometric elements (curves and tangents) is the design speed of the elements. Many researches have demonstrated that the design speed does not correspond to the real speed, particularly along curves with sharp radii of two-lane rural roads. Another important hypothesis of the procedure regards the speed variation model and the acceleration/deceleration rates. In particular, the model considers the constant speed along the circular curves; the driver accelerates towards the maximum design speed as soon as he exits from a circular curve and he starts the deceleration just in time to finish it at the point of curvature of the curve ahead. To improve the reliability of this consistency check this design speed-profile should be replaced by a new model that better represents the real speed-profile. Therefore, this new model should use the operating speed instead of the design speed.

The regression equations that correlate the characteristics of the horizontal curves with the operating speed (V85) and the general characteristics of the horizontal alignment (CCR and width) with the maximum speed reached on long tangents (environmental speed) were already developed by a previous research (Crisman B., Marchionna A., Perco P., Robba A., Roberti R., 2005). With the availability of acceleration and deceleration models that respect real driver behaviour, it will be possible to develop an operating speed-profile model that represents the real speed-profile along a horizontal alignment. Consequently, this operating speed-profile will be used to check more effectively the consistency of the road alignment.

The object of this research is to establish conclusively deceleration/acceleration rates, and driver speed behaviour approaching/departing from curves and along short tangents. In fact, the first indications were already collected: the driver decelerates along the spiral curve (Perco P., Crisman B., 2004) and the deceleration continues inside the circular curve (Perco P., 2005). The first step in the research involved the collection of a sample of speed-data to define the best procedures to collect data and to process them. In particular, these data were collected to evaluate the reduction in speed approaching a circular curve because, given the nature of curve-related accidents, accurate deceleration rates are more important in the model than acceleration rates.

ACCELERATION-DECELERATION RATES IN PREVIOUS RESEARCHES

The research studied the acceleration and deceleration rates of vehicles approaching and departing from curves beginning from the fifties (Taragin A., 1954; Holmquist C., 1970). However, in that period there was no effective equipment and the data collected were not sufficient to establish conclusively acceleration and deceleration rates. Moreover, at that time these rates were not of particular interest because there was no useful procedure in the design process that used them. The Swiss standard (Swiss Association of Road Specialists, 1981) was the first standard to introduce a design speed-profile model to evaluate the design consistency by predicting speed reduction between successive design horizontal elements. This model assumes that acceleration/deceleration occurs on the approach/departure tangents and on spirals curves and, therefore, that speed is constant through the circular curve. The Swiss standard model uses a constant deceleration and acceleration rates of $0,80 \text{ m/s}^2$. The new Italian standard (Ministry of Infrastructures and Transportation, 2001) uses the same design speed-profile model as the Swiss standard for consistency evaluation of the horizontal alignment. After the introduction of the operating speed, Lamm proposed an operating speed-profile model to evaluate the design consistency (Lamm R., Choueiri E.M., 1987). Deceleration and acceleration rates for this model came from Lamm, Choueiri and Hayward (Lamm R., Choueiri E.M., Hayward J. C., 1988), who collected speed data using a car-following technique. The study involved six curves that had posted advisory speed plates ranging from 48,3 to 64,4 km/h. 11 sections, at 75 m intervals, were marked along the roads investigated from tangent to the curve (deceleration) and from the curve to the tangent (acceleration). The speeds of at least 20 passenger cars were recorded at each of the 11 test sections. The results of the study clearly indicated that the acceleration ends and the deceleration begins at about 210 m to 230 m from the end of the observed curve sections. The average deceleration and acceleration rates ranged between $0,85$ and $0,88 \text{ m/s}^2$. Since the difference was small, Lamm selected an average acceleration and deceleration rate of $0,85 \text{ m/s}^2$ for the operating speed-profile model. At the end of the eighties, another two German studies obtained deceleration rates. Steierwald and Buck (Steierwald, G., Buck M., 1992) used the radar car-following technique on four road sections to relate the speed behaviour with constructional, operational and traffic conditions. The authors reported an average deceleration rate of $0,23 \text{ m/s}^2$ before speed limit signs and a deceleration rate between $0,40 \text{ m/s}^2$ and $0,60 \text{ m/s}^2$ before of signs with the names of places. Kockelke and Steinbrecher (Kockelke W., Steinbrecher J., 1987) studied the speed-profile of vehicles entering 22 built-up areas. They reported a deceleration rate normally less than

1,00 m/s² before signs with the names of places, even if they surveyed deceleration up to 2,50 m/s². Krammes et al. (Krammes R.A., Brakett R. Q., Shaffer M. A., Ottesen J. L., Anderson I. B., Fink K. L., Collins K. M., Pendleton O. J., Messer C. J., 1995) used the acceleration and deceleration rates reported by Lamm et al. (Lamm R., Choueiri E.M., Hayward J. C., 1988) for the preliminary operating speed-profile model to serve as the basis for the design consistency module of Interactive Highway Safety Design Module (IHSDM). Afterwards, Krammes and Collins decided to confirm these assumptions (Collins K.M., Krammes R.A., 1996). Therefore, the authors collected limited but detailed speed data to establish deceleration and acceleration rates approaching and departing from curves. The data were collected along 10 curves (175 m ≤ R ≤ 437 m; 94 m ≤ L ≤ 245 m) and the approach tangents (260 m ≤ L ≤ 1393 m). The speed was collected with a series of seven infrared photoelectric sensors placed along one approach/departure tangent and half of the horizontal curve at regular intervals. The sample size of free-flow passenger cars ranged from 26 to 103 vehicles for each curve and direction. The acceleration and deceleration rates were calculated using the observed operating speed at the endpoints of the intervals and the lengths of the intervals. The acceleration rate between the different sites ranged between 0,12 m/s² and 0,52 m/s², while the deceleration rate between 0,35 m/s² and 1,19 m/s². The conclusion was that the observed deceleration rate was not significantly different from the rate 0,85 m/s² assumed in the model, while the assumed acceleration rate may overestimate real acceleration. However, Hirshe (Hirshe M., 1987) previously hypothesized that the use of the operating speed for evaluating design consistency tended to underestimate speed reduction experienced by individual drivers. In fact, even if the use of the operating speed in the design consistency check is reasonable, the reduction in the operating speed from an approach tangent through a horizontal curve could not provide an accurate representation of the real driver speed reduction. Consequently, McFadden and Elefteriadou (McFadden J., Elefteriadou L., 2000) conducted a new study to assess the implications of using the operating speed for evaluating design consistency. The vehicle speeds were collected at 21 curves (175 m ≤ R ≤ 875 m; 76 m ≤ L ≤ 531 m) and along the approach/departure tangents (153 m ≤ L ≤ 723 m). Speeds were collected using light detecting and ranging (lidar) guns. At each site, speed data for at least 72 free-flow passenger cars were collected. The research confirmed the Hirshe's hypothesis that the use of the operating speeds to evaluate the design consistency underestimates the speed reduction experienced by the individual drivers. Consequently, the authors proposed a new model that uses the speed reduction experienced by 85 percent of the driver population to evaluate the consistency of the alignment, but they did not present new acceleration and deceleration rates. Fitzpatrick et al. (Fitzpatrick K., Elefteriadou L., Harwood D., Collins J., McFadden J., Anderson I., Krammes R., Irizarry N., Parma K., Bauer K., Passetti K., 2000) used the data of McFadden and Elefteriadou (McFadden J., Elefteriadou L., 2000) to develop the acceleration and deceleration rates assumed in the formulation of the speed-profile model of the IHSDM design consistency module. After the correction of the speed data to account for the cosine error, speeds measurements were interpolated to obtain the speeds at the following sections: the beginning and the end of the curve; one-quarter, one-half, and three-quarter distances within the curve; 50 m increments up to 200 m beyond either end of the curve. The authors considered two different approaches in calculating the acceleration rates: estimating the average acceleration and deceleration rate for each vehicle and then calculating the 85th percentile rate of these average rates, or calculating the operating speeds at each section and then calculating the acceleration and deceleration rates. The second approach was selected, since it would correspond to the operating speed-profile. The results showed that the acceleration and deceleration rates of 0,85 m/s² used in the original model are significantly different from the rates observed. The acceleration model proposed for the speed-profile is a step function based on the curve radii (0,00 m/s² R > 875 m; 0,21 m/s² 436 m < R ≤ 875 m; 0,43 m/s² 250 m < R ≤ 436 m; 0,54 m/s² 175 m < R ≤ 250 m), while the deceleration model is a linear regression for a limited group of radii ($|0,6794 - 295,14/R|$ 175 m ≤ R < 436 m), and a constant rate for the other radii (0,00 m/s² R ≥ 436 m; 1,00 m/s² R < 175 m). The model presents an inconsistency because the radius for which the deceleration rate is zero does not correspond to the radius for which the acceleration rate is zero. Moreover, the speed data were not collected along sharp curves where the speed reduction is more important for safety (there are only two curves with a radius of 175 m and two with a radius of 250 m) and, consequently, the deceleration rate could not represent real driver behaviour before these curves. Finally, this short review shows that the previous researches have not collected sufficient data to establish conclusively deceleration and acceleration characteristics, especially for sharp curves where the speed reduction is more important to safely traverse the curve.

DATA COLLECTION

The device used to collect the data is a Light Detection and Ranging (Lidar) gun. Lidar is a multi-purpose tool that has become increasingly popular as an alternative to conventional radar speed guns. The use of Lidar has two major advantages over radar. First, it can measure distances to a vehicle as well as the speed of the vehicle. The second advantage is that the signal transmitted by Lidar travels in a straight line as opposed to the conical patterns of radar transmission, making it easier to pinpoint the vehicle. The information that the Lidar device provides (distance and speed) enables the speeds of individual vehicle to be measured at known location along the road. The Lidar gun used in this study is similar to the device used by the police in speed enforcement, except that it has an increased range of 1.200 m. However, the maximum distance at

which a speed measurement can be made is about 800÷900 m because if the distance is larger the car is too small in the sighting scope and, consequently, it is not possible to pinpoint it with the red aiming dot. The Lidar device used in this research measures distances with an accuracy of ± 15 cm (speed mode) and speeds with an accuracy of ± 2 km/h. When the target-vehicle is aimed and the trigger is pressed a low growl begins, indicating the instrument is trying to acquire a lock on the target. The instrument utters a beep when the vehicle speed is captured. The Lidar gun does not have a memory so it has to be connected with a computer where the data are stored. Even though there is the possibility of carrying out continuous measures until the trigger is released with a specific computer program, practical experience suggests that it is advisable to use the single measures method. The Lidar gun has to be mounted on a tripod, especially if the measuring distance is long.

The Lidar gun measures only the speed component along its axis, so it is important to place the gun in the direct path of the vehicle. Otherwise, the cosine error occurs and the speeds measured must be corrected. Moreover, it is important to hide the Lidar gun with the tripod, the computer and the operator from oncoming traffic in order to minimize the effects of their presence on the driver and, consequently, on the speed data. Figure 1 shows a measuring place.



Figure 1: Measurement hiding place with the Lidar gun on the tripod and the computer

In positioning the Lidar gun two different places were considered, as showed in figure 2. The first (figure 2-A) was in front of the vehicles surveyed, the second (figure 2-B) was behind the vehicles surveyed. The first place has the advantage that the vehicle is nearest when it is entering the curve and the speed variation has maximum rate, but it requires a good hiding-place. The second place can be used efficiently when there is no hiding-place near the observed curve, but it has the important disadvantage that if the surveyed car is covered by a following vehicle the speed measurements near the curve are lost.

For the speed measurement, the Lidar gun was aimed at the vehicle's most reflective point, preferably the license plate or the bumper. The vehicle speed measurements were collected starting at the maximum possible distance, and ending along the curve, when the target-vehicle goes out of the line of sight.

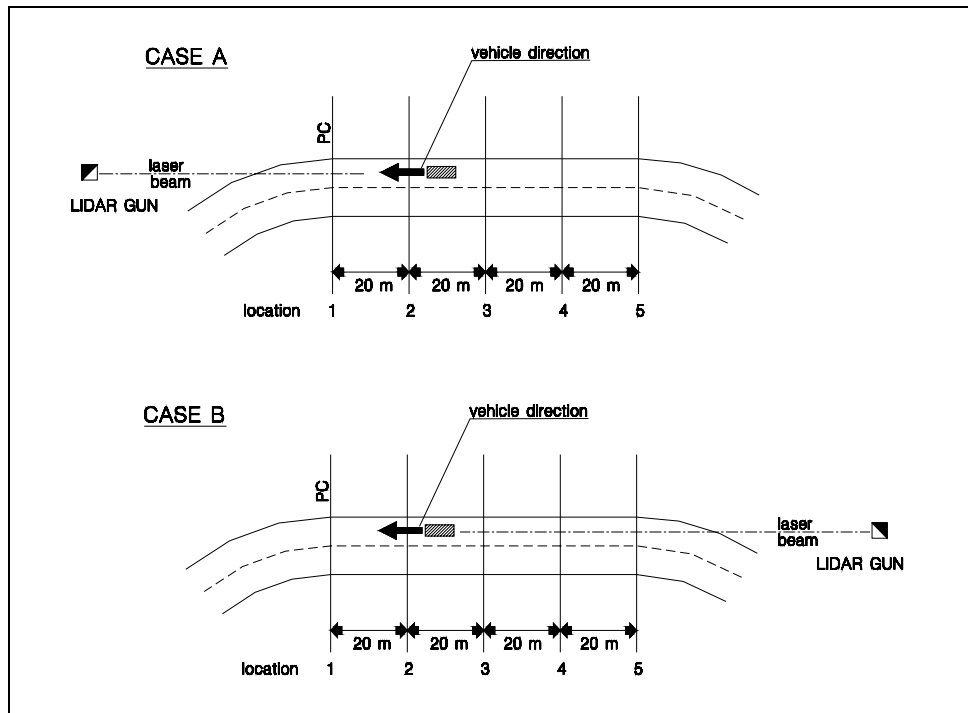


Figure 2: The two possible positions of the Lidar gun

Speed data were collected on 10 sites composed of a curve and the preceding tangent on six two-lane rural roads in the north-east of Italy. Table 1 gives a summary of the geometric characteristics of the sites. The curves do not have a spiral transition. The overall road environment of the surveyed sections is flat or hilly terrain. All the roads have the usual cross sections of Italian two-lane rural roads, with two lanes ($3,25 \leq \text{lane width} \leq 3,75 \text{ m}$) and, in some cases, two paved shoulders ($0 \leq \text{shoulder width} \leq 1,50 \text{ m}$). The width in table 1 is the total width of the road (carriageway+shoulder). The longitudinal slope never exceeds $\pm 3,0\%$. The curves and the preceding tangent do not present characteristics that could affect the driver and limit available sight distance, with the exception of site 10. In fact, along this curve there is a central physical island of a minor road intersection. Probably, the presence of this physical island at the beginning of the curve affects the speed, leading the driver to reduce the speed below the value normally accepted for this curve radius. Most sites are characterized by sharp radii (average radius 169 m; $15 \text{ m} \leq R \leq 515 \text{ m}$) because the object of the research was to obtain a deceleration rate used by the driver on curves where a real speed reduction is needed to travel the curve safely. These curves for two-lane rural roads have radii lower than $250 \div 300 \text{ m}$ (Barjonet P., Lagarde D., Serveille J., 1992). Moreover, these results could complete those of the study of Fitzpatrick et al. (Fitzpatrick K. et al., 2000) that used curves with higher radii (average radius 432m; $175 \text{ m} \leq R \leq 873 \text{ m}$). Vehicles surveyed had a minimum 5 seconds of headway to ensure that they were not impelled. Only the speeds of passenger cars were measured. At each site, speed data were collected for a minimum of 100 vehicles. Table 1 shows the average number of vehicles for each measurement location after data reduction. Data were collected during daylight, on a dry road. The traffic never exceeded 420 vehicles/hour (site 7) during data collection.

Tab 1: Geometric characteristics of the sites

Site	Road	Curve radius	Curve Length	Tangent length	Previous curve radius	Grade	Width	Vehicles
		[m]	[m]	[m]	[m]	[%]	[m]	
1	SP35 TS	280	93	790	1500	-2,88	12,00	51
2	SP1 TS	150	96	240	75	1,23	7,30	168
3	SS58	14	42	100	150	-2,82	10,50	108
4	SP6 TS	100	53	140	300	-2,29	7,00	65
5	SS58	60	88	78	270	2,31	10,50	90
6	SP19 GO	320	294	784	385	0,05	7,30	134
7	SP19 GO	520	376	650	700	-0,38	7,30	121
8	SS55	80	53	192	54	1,22	7,30	67
9	SS55	54	65	192	80	-1,22	7,30	62
10	SS55	175	183	1096	275	0,10	7,40	131

ANALYSIS METHOD

Not all the sites investigated had speed-data along the curve. In particular, it was difficult to collect speeds along the curves of the sites where the Lidar gun was hidden in front of the vehicles near the curve (sites, 2, 3, 6, 9). Consequently, the data-analysis was conducted along the tangent starting from the point of curvature. However, the available data along the curves (sites 1, 4, 5, 7, 8, 10) were calibrated to account for the cosine error. This error occurs when the speeds are not measured in the direct path of the vehicle. In this case, the ratio of the Lidar speed reading to the true forward speed of the vehicle is equal to the cosine of the angle between the Lidar and the vehicle's direction of travel. On tangents, where the Lidar gun can measure speeds in or near the vehicle path, the cosine error is zero, or negligible. For vehicles on a horizontal curve, the angle between the laser beam and the vehicle's forward direction changes constantly through the curve. These corrected data along the curve confirmed the results of Perco (Perco P., 2005) that the deceleration continues inside the curve, even if the maximum deceleration rate was observed just before the point of curvature. A problem that could arise for this correction is that the real path of the vehicle is not known, especially when it enters sharper curves, during steering action. In this situation the real path may be very different from the road axis (Perco P., 2005) and, consequently, the angle between the road axis and the laser beam does not correspond to the angle between the vehicle path and the laser beam.

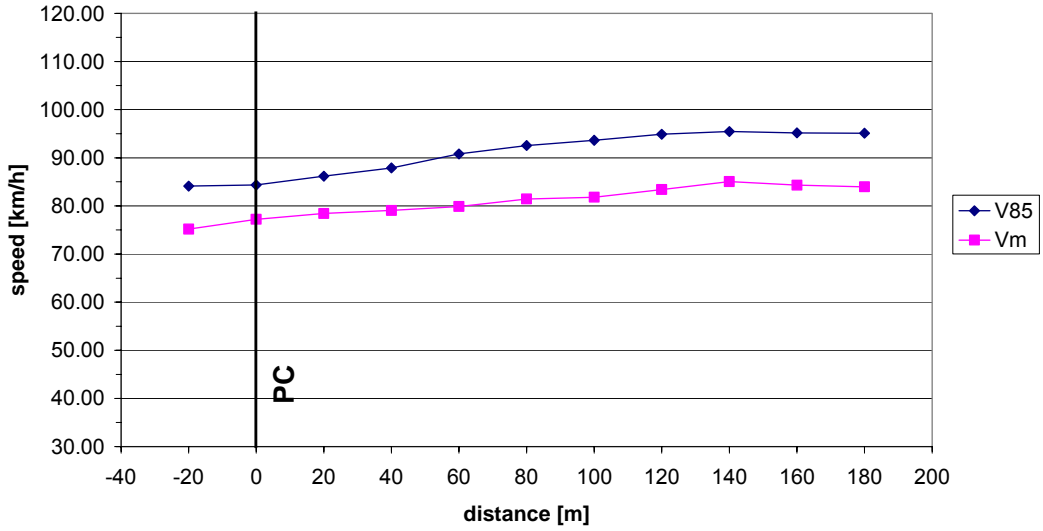
Starting from the point of curvature, the tangent before the curve was divided into intervals of 20 m and the speed of each vehicle was calculated at each location. Vehicle speeds were determined by interpolating between the closest speed measurements on either side of the location. Observed average and operating speeds were plotted for all the sites (figure 3). These speed-profile plots are of three different types, as is shown in figure 4, and this difference depends on the length of the upstream tangent. In the first case the tangent is long and a constant speed can be reached and maintained by the driver (sites 1, 4, 6, 7, 10). This speed could be considered as the environmental speed of the road (Crisman B., Marchionna A., Perco P., Robba A., Roberti R., 2005). In the second case the tangent is not long enough to reach the environmental speed (sites 2, 8, 9). The driver accelerates from the previous curve and then decelerates for the next curve. In the third case the driver starts the deceleration before the first measurement location (sites 3, 5). The first type is the best case for study but it is difficult to find sharper curves preceded by a very long tangent. So, to measure deceleration rates before curves with smaller radii, also sites of the second and third type were used.

The deceleration rate was calculated along the distance L between the point of curvature (PC) and a location which was determined for each type of site in a different way. For the first type, the average approaching speed was calculated on a 100 m section along the tangent, where a constant speed was maintained. However, this section ends at least 200 m before the PC. Consequently, a single sample t-test was conducted at each location to determine which is the farthest location from the point of curvature having the mean of the speed distribution which statistically does not differ from this average approaching speed (p -value 0,05). The deceleration begins from this location. For the second type of sites, the t-test was conducted to determine which is the farthest location from the point of curvature having the mean of the speed distribution which is not statistically different from the maximum mean speed observed in all the locations. Finally, for the third type of sites, this location always corresponds to the first location surveyed. The distance L is shown in tables 2 and 3.

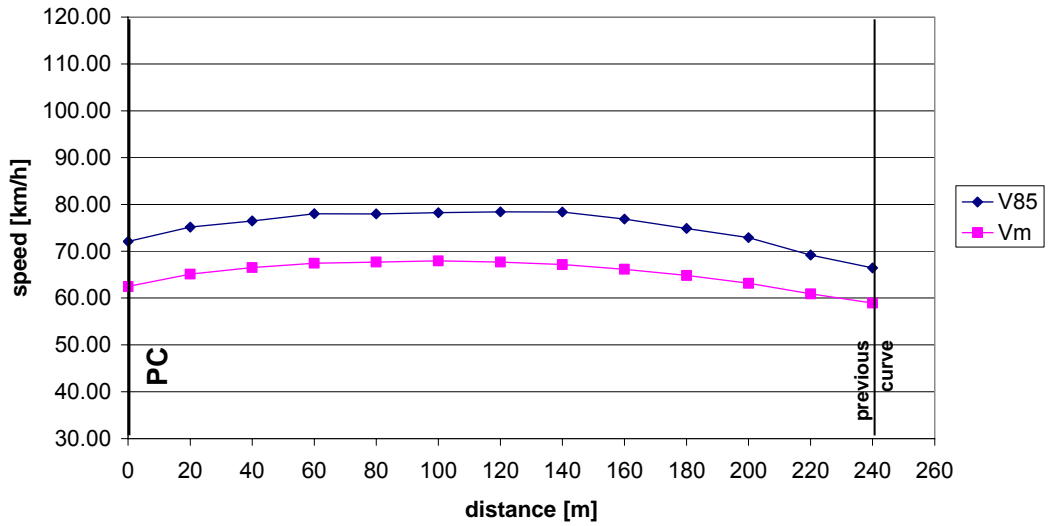
The typical speed distribution is shown in figure 5 (site 6). There are different shapes for the speed-distributions because the speeds on the curve usually have less variability than on the approach tangent. The speeds along the tangent are more dispersed because the driver chooses freely the speed (lower and wider speed distribution) but along the horizontal curve the speed choice is more constrained by the geometric characteristics of the curve (higher and narrower speed distribution).

To calculate the deceleration rates from tangent to curve two approaches were taken into consideration. The first approach involved the calculation of the average and the operating speeds at each location and, consequently, the deceleration rate was calculated directly from these speeds. In the second approach, the deceleration rate was calculated at each location for each vehicle and then the average and the 85th percentile rates were calculated. However, the deceleration rate obtained from the average speed (first approach) and the average deceleration rate (second approach) were not used in the continuation of the analysis. In fact, the objective of this research was to develop a deceleration model that can be used in the operating speed-profile model. Consequently, as made in the model developed for the IHSDM (Fitzpatrick K. et al., 2000), only the deceleration rates obtained from the operating speed and the 85th percentile of the deceleration rates of all vehicles were considered.

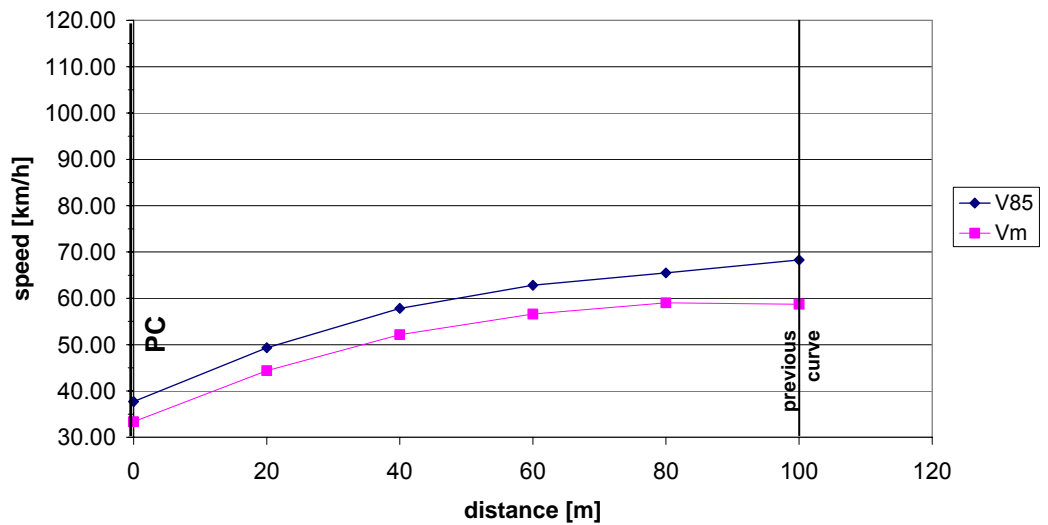
site 1 - SP 35



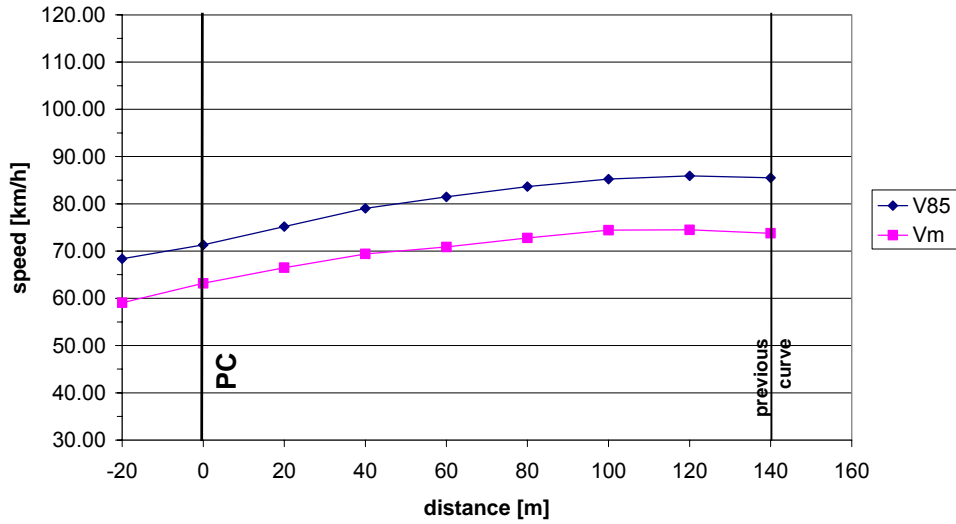
site 2 - SP1



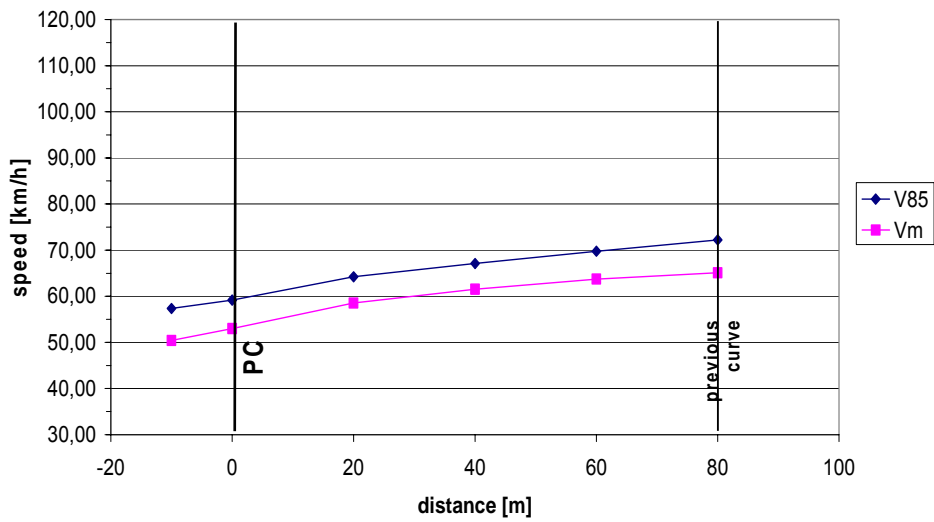
site 3 - SS58



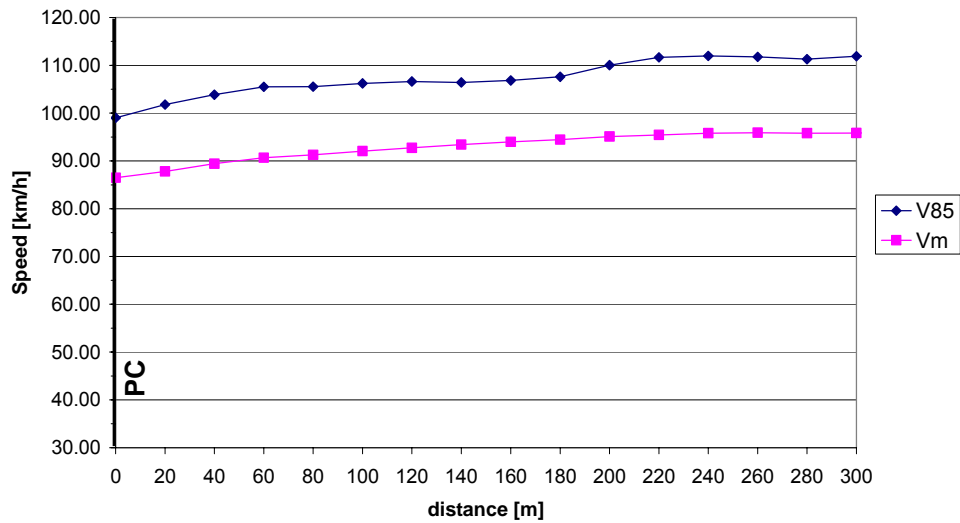
Site 4 - SP6



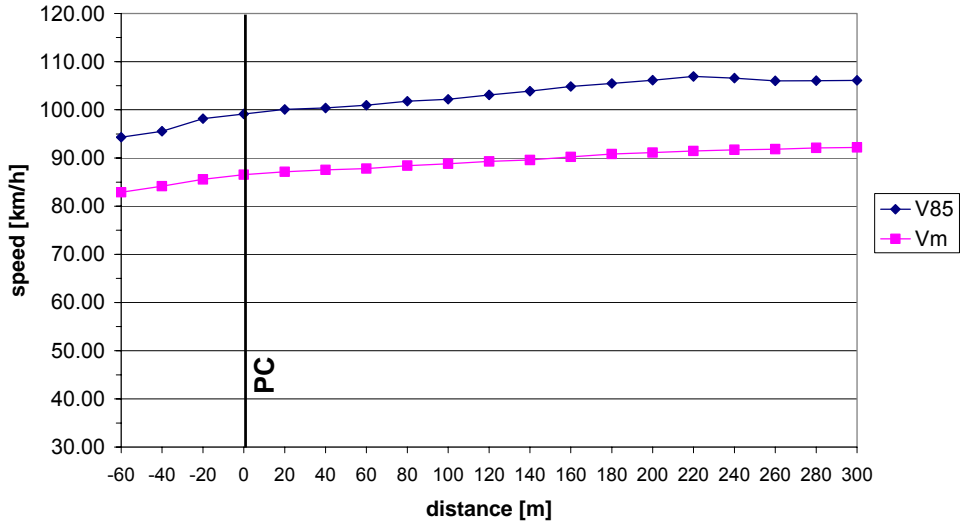
Site 5 - SS58



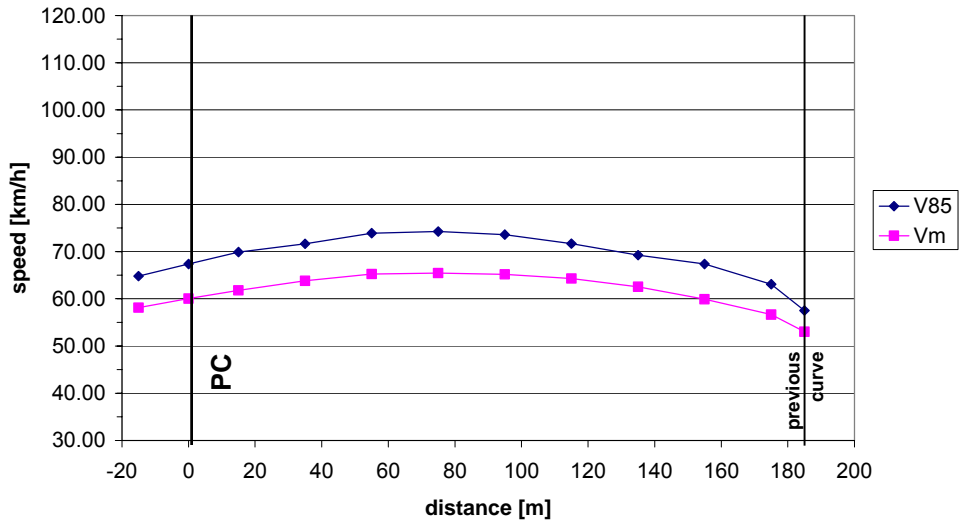
Site 6 - SP19



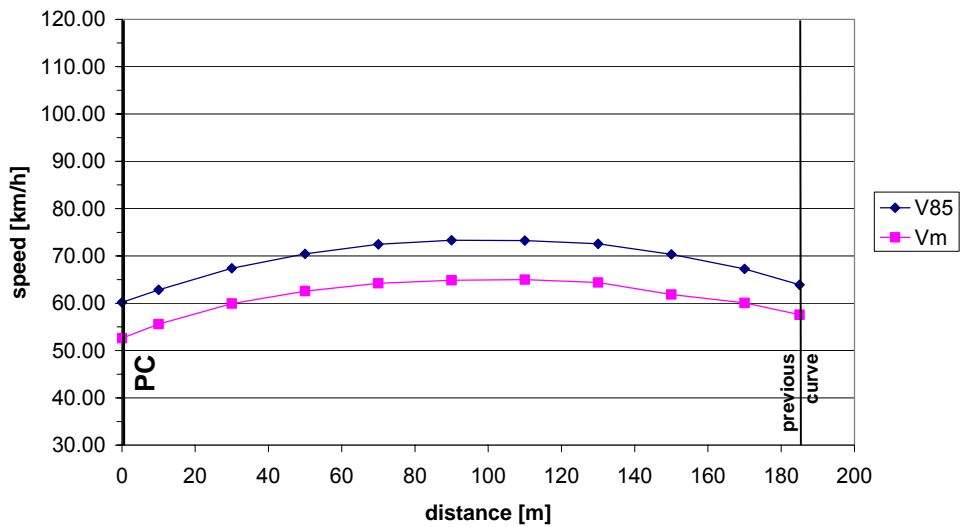
Site 7 - SP19



Site 8 - SS55



Site 9 - SS55



Site 10 - SS55

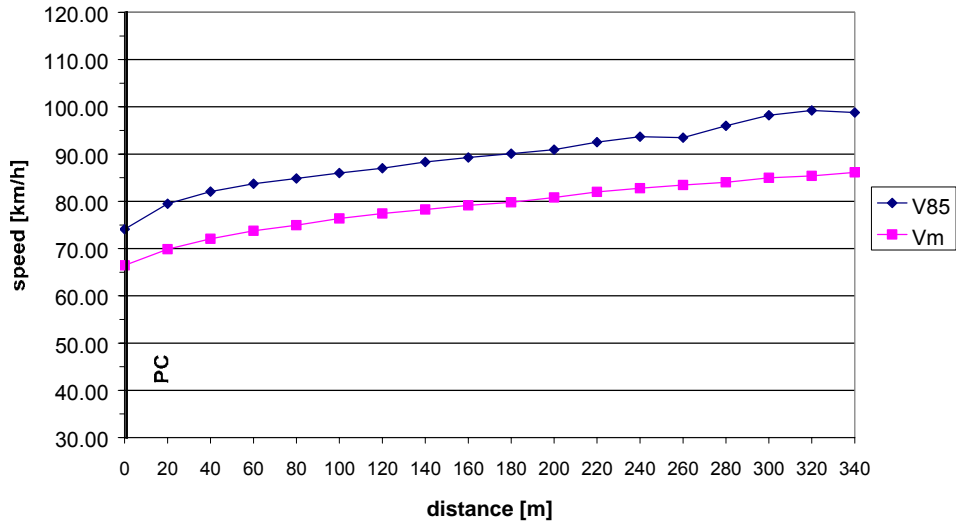


Figure 3: The speed-profile plots

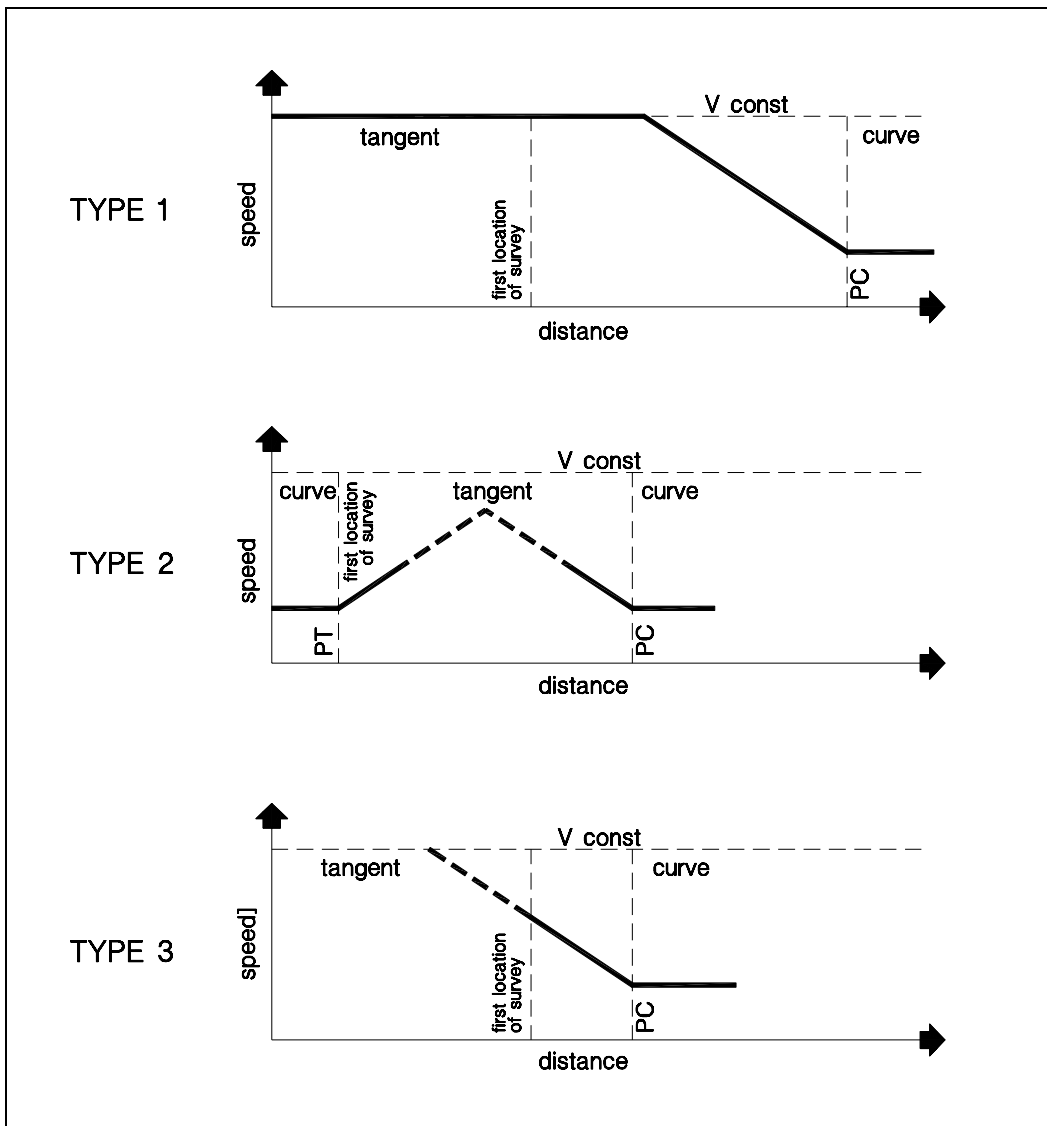


Figure 4: The different types of speed-profile plots

RESULTS

The first analysis approach involved the calculation of the average and operating speeds at each location. Table 2 shows the average speeds, while table 3 shows the operating speeds. The distance L in tables 2 and 3 is the distance between the point of curvature and the location where the maximum speeds $V_{m_{max}}$ and $V_{85_{max}}$ during the deceleration action were reached. $V_{m_{min}}$ and $V_{85_{min}}$ are the minimum speeds observed at a location inside the distance L and they always correspond to the speed on the point of curvature. ΔV_m and ΔV_{85} are the differences between the previous speeds. The average ΔV_m is 9,82 km/h for all sites, while the average ΔV_{85} is 11,68 km/h. The deceleration rates dm_{V_m} and $dm_{V_{85}}$ are calculated from the previous differences of speeds along the distance L , presuming a uniformly decelerated motion. The average dm_{V_m} for all sites is 0,54 m/s², while the average $dm_{V_{85}}$ is 0,71 m/s². $dmax_{V_m}$ and $dmax_{V_{85}}$ are the maximum deceleration rates observed between two successive locations inside the distance L , while $dmin_{V_m}$ and $dmin_{V_{85}}$ are the minimum deceleration rates observed between two successive locations.

Tab 2: Observed average speeds and calculated deceleration rates

Site	L	$V_{m_{max}}$	$V_{m_{min}}$	ΔV_m	dm_{V_m}	$dmax_{V_m}$	$dmin_{V_m}$
	[m]	[km/h]	[km/h]	[km/h]	[m/s ²]	[m/s ²]	[m/s ²]
1	80	81.45	77.21	4.24	0.32	0.49	0.19
2	40	66.52	62.46	4.06	0.50	0.65	0.36
3	100	59.03	33.37	25.66	1.14	1.65	0.54
4	80	72.76	63.17	9.59	0.63	0.83	0.40
5	80	65.10	53.00	12.10	0.69	1.19	0.34
6	140	93.40	86.49	6.91	0.34	0.56	0.21
7	120	89.27	86.54	2.73	0.16	0.20	0.09
8	40	63.81	60.06	3.75	0.51	0.54	0,49
9	80	64.21	52.61	11.60	0.76	1.39	0.40
10	280	84.04	66.46	17.58	0.37	0.92	0.19
average	104	73.96	64.14	9.82	0.54	0.84	0.30

Tab 3: Observed operating speeds and calculated deceleration rates

Site	L	$V_{85_{max}}$	$V_{85_{min}}$	ΔV_{85}	$dm_{V_{85}}$	$dmax_{V_{85}}$	$dmin_{V_{85}}$
	[m]	[km/h]	[km/h]	[km/h]	[m/s ²]	[m/s ²]	[m/s ²]
1	80	92.54	84.36	8.18	0.70	1.01	0.58
2	40	76.49	72.08	4.41	0.63	0.87	0.39
3	100	68.28	37.71	30.57	1.25	1.95	0.66
4	80	83.66	71.30	12.36	0.92	1.15	0.23
5	80	72.23	59.19	13.04	0.83	1.20	0.68
6	140	106.40	99.02	7.38	0.42	1.07	-0.09
7	120	103.08	99.15	3.93	0.26	0.36	0.12
8	40	71.66	67.38	4.28	0.66	0.89	0.48
9	80	72.44	60.16	12.28	0.91	1.42	0.56
10	280	94.41	74.09	20.32	0.47	1.65	-0.07
average	104	84.12	72.44	11.68	0.71	1.16	0.35

The deceleration rates calculated from the average speed is always lower than those calculated from the operating speed because the ΔV_m is always lower than ΔV_{85} . This is in accordance with the different shapes of the speed distributions (figure 5) that draw closer to the average speed as the distance from the curve decreases.

In the second analysis approach the deceleration rate was calculated for each vehicle along each interval of 20 m between two successive locations inside the distance L . Consequently, the average and the 85th percentile deceleration rates were calculated for each interval. Table 4 shows the average deceleration rates dm_{sv} and $d85_{sv}$ along the distance L , the maximum deceleration rates observed between two successive locations inside the distance L dmm_{sv} and $d85m_{sv}$, and the minimum deceleration rates observed between two successive locations inside the distance L dmm_{sv} and $d85m_{sv}$. The average dm_{sv} for all sites is 0,53 m/s², while the average $d85_{sv}$ is 0,86 m/s². In calculating the deceleration rate for each vehicle, it was noted that some vehicles reached a deceleration rate of 4,00 m/s² just before the curves with lower radii, and many vehicles exceeded the rate of 2,00 m/s².

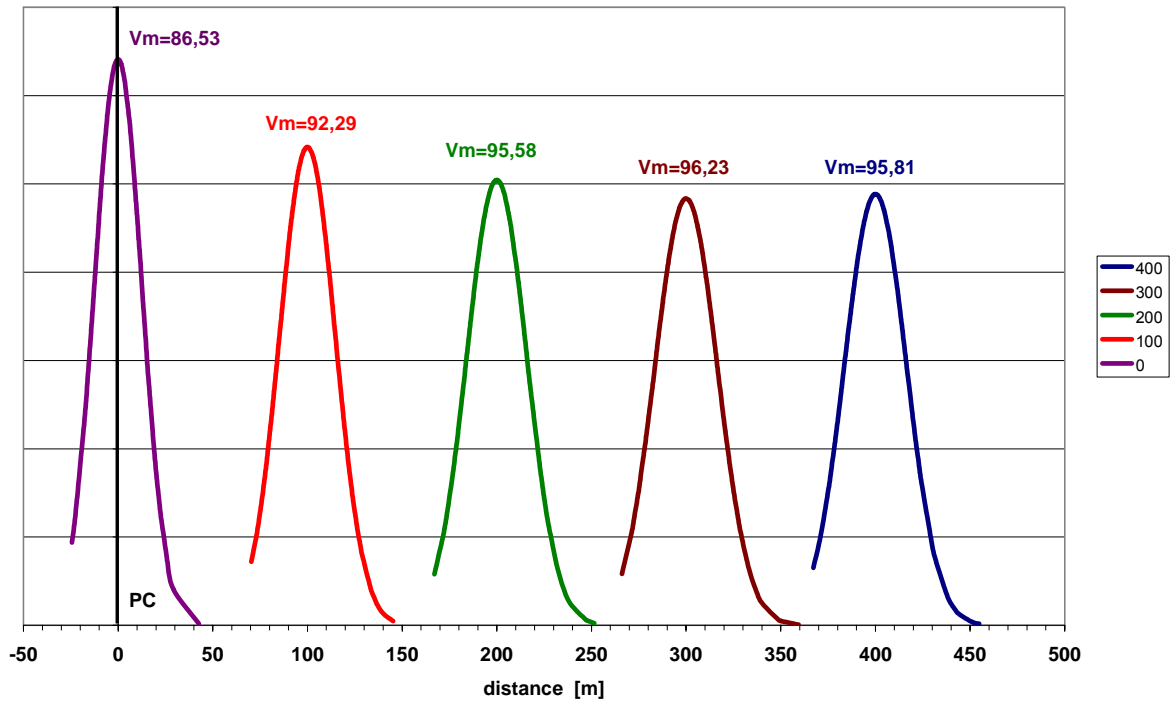


Figure 5: The Speed distributions along the tangent (site 6)

Tab 4: Observed deceleration rates

Site	Average			85 th percentile		
	dm_{sv} [m/s ²]	$dmmax_{sv}$ [m/s ²]	$dmin_{sv}$ [m/s ²]	$d85_{sv}$ [m/s ²]	$d85max_{sv}$ [m/s ²]	$d85min_{sv}$ [m/s ²]
1	0.25	0.28	0.23	0.49	0.51	0.46
2	0.22	0.24	0.19	0.48	0.50	0.47
3	1.16	1.57	0.64	1.37	2.00	0.52
4	0.70	0.97	0.47	1.20	1.59	0.91
5	0.67	0.98	0.34	0.99	1.27	0.62
6	0.33	0.47	0.25	0.68	0.87	0.56
7	0.22	0.31	0.15	0.57	0.73	0.43
8	0.55	0.58	0.52	0.86	0.97	0.76
9	0.86	1.31	0.41	1.31	2.01	0.66
10	0.32	0.48	0.22	0.65	0.83	0.49
average	0.53	0.72	0.34	0.86	1.13	0.59

The second analysis approach leads to higher deceleration rates than the first one. Therefore, assuming that the two deceleration data were dependent because were calculated from the same speed data, a paired t-test was performed, to determine whether the average deceleration rates calculated with the two different approaches were significantly different from each other. The Null Hypothesis was that the average deceleration rate dm_{V85} was equal to the average deceleration rate $d85_{sv}$. The results of the t-test, summarized in table 5, indicate that the two deceleration rates are statistically different at a significance level of 0,05. The two approaches result in different deceleration rates and, consequently, one of them should be chosen for the development of a final deceleration model. The deceleration rates used in the actual speed-profile IHSDM model are calculated with the first approach. The reason suggested in the report (Fitzpatrick K. et al., 2000) is that those rates would correspond to the operating speed-profile.

Two single-sample t-tests were performed to determine whether the average calculated deceleration rates dm_{V85} and $d85_{sv}$ were different from the rate proposed by Lamm et al. (Lamm R., Choueiri E.M., Hayward J. C., 1988) and Krammes et al. (Krammes R. et al., 1995) for the operating speed-profile (0,85 m/s²). The results of these t-tests, also summarized in table 5, indicate that dm_{V85} is statistically different from 0,85 m/s² at a significance level of 0,05, while $d85_{sv}$ is not statistically different. These results confirm that the deceleration rate of 0,85 m/s² is significantly different from the rate observed, as proved by Fitzpatrick et al.

(Fitzpatrick K. et al., 2000), but only if this rates is calculated from the operating speed. On the contrary, if the deceleration rate is calculated as the 85th percentile of decelerations of each vehicle, a rate 0,85 m/s² could be a good approximation.

Tab 5: Tests of deceleration rates

test	Null hypothesis H ₀	mean [m/s ²]		standard deviation [m/s ²]		number of cases (n)		t	p - value	reject H ₀ ?
		Sample 1	Sample 2	Sample 1	Sample 2	Sample 1	Sample 2			
1	$dm_{V85} = d85_{sv}$	0.705	0.860	0.287	0.339	10	10	-2.519	0.033	Yes
2	$dm_{V85} = 0.85 \text{ m/s}^2$	0.705	-	0.287	-	10	-	-1.596	0.045	Yes
3	$d85_{sv} = 0.85 \text{ m/s}^2$	-	0.860	-	0.339	-	10	0.093	0.928	No
4	$dm_{V85} (L) = dm_{V85} (40)$	0.705	0.944	0.287	0.451	10	10	-2.530	0.032	Yes
5	$d85_{sv} (L) = d85_{sv} (40)$	0.860	1.043	0.339	0.503	10	10	3.208	0.011	Yes

Sample 1	test 1-2-4: $dm_{V85} (L)$	test 3-5: $d85_{sv} (L)$
Sample 2	test 1: $d85_{sv} (L)$	test 4: $dm_{V85} (40)$ test 5: $d85_{sv} (40)$

The considerable differences between the maximum and the minimum deceleration rates in tables 2, 3, 4 suggest that the driver reduces speed in different ways as he approaches the curve. Normally, the observed deceleration rate increases as the distance from the point of curvature decreases. Probably, the driver in the first phase raises his foot from the accelerator and, in the second phase, applies the brake. For example, figure 6 shows the deceleration rates for each location of site 4. In particular, the results of this analysis show that the maximum deceleration reached before the curve is much higher than the average deceleration rate.

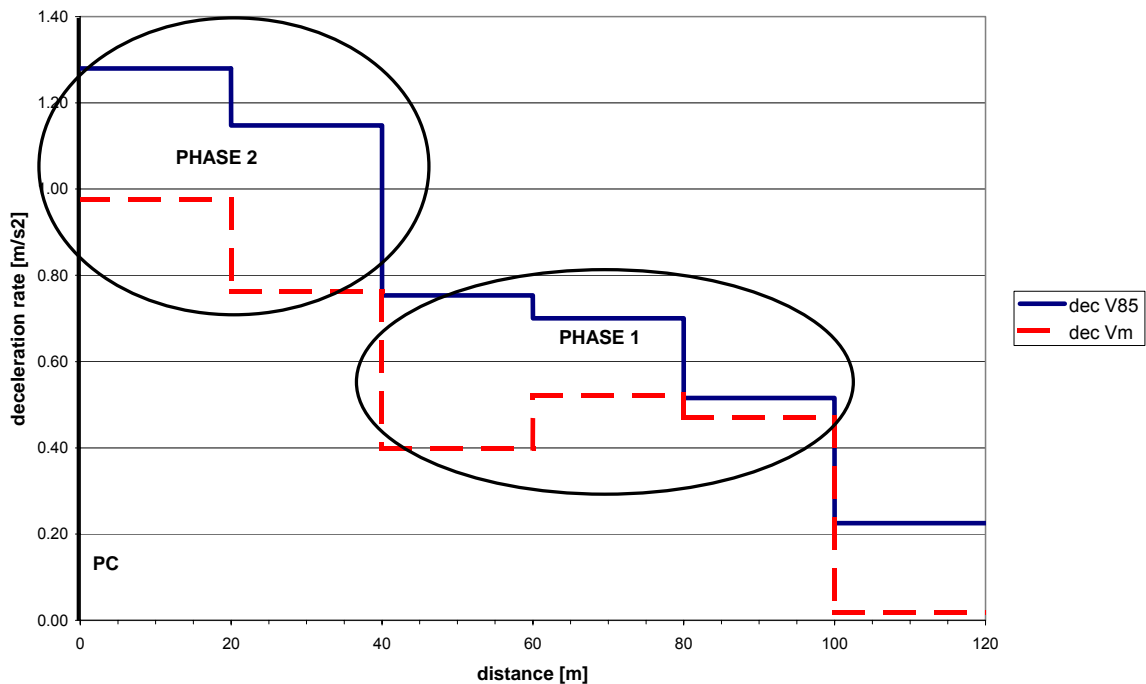


Figure 6: The deceleration rates along the tangent (site 4)

Consequently, a second analysis limited to the final 40 m before the point of curvature was carried out to investigate the deceleration rate reached when the brake is applied. The distance of 40 m is the result of an

examination of the speed-profile plots of all sites. Table 6 shows the same previous variables calculated along a distance that begins on the tangent 40 m upstream from the point of curvature. Obviously, also in this case the deceleration rate calculated from the average speed is lower than that calculated from the operating speed and the deceleration rate calculated with the second approach is higher than that calculated with the first approach. The average $d85_{sv}$ for all sites is $1,04 \text{ m/s}^2$, while the average dm_{v85} is $0,94 \text{ m/s}^2$. These values are higher than the average deceleration rates along all the distance L . Assuming that the two deceleration data were dependent because they were calculated from the same speed data, a paired t-test was performed to determine whether the average deceleration rates calculated along the entire distance L were statistically different from the average deceleration rates calculated along the final 40 m. The results of the t-test, summarized in table 5, indicate that the two deceleration rates are statistically different at a significance level of 0,05. These results confirm that the deceleration rate is not constant along the entire distance travelled during the speed reduction but it varies along it and this can be schematized at least in two parts characterized by the way the driver behaves.

Tab 6: Observed and calculated average deceleration rates along 40 m

Site	Vm_{max}	Vm_{min}	ΔVm	dm_{Vm}	dm_{sv}
	[km/h]	[km/h]	[km/h]	[m/s ²]	[m/s ²]
1	79,05	77,21	1,84	0,28	0,27
2	66,52	62,46	4,06	0,51	0,22
3	52,15	33,37	18,78	1,55	1,48
4	69,4	63,17	6,23	0,80	0,88
5	61,52	53	8,52	0,94	0,9
6	89,42	86,49	2,93	0,50	0,44
7	87,55	86,54	1,01	0,17	0,28
8	63,81	60,06	3,75	0,51	0,55
9	59,94	52,61	7,33	1,06	1,17
10	72,06	66,46	5,60	0,75	0,45
average	70,14	64,14	6,01	0,71	0,66

Tab 7: Observed and calculated 85th percentile deceleration rates along 40 m

Site	$V85_{max}$	$V85_{min}$	$\Delta V85$	dm_{v85}	$d85_{sv}$
	[km/h]	[km/h]	[km/h]	[m/s ²]	[m/s ²]
1	87,87	84,36	3,51	0,58	0,51
2	76,49	72,08	4,41	0,63	0,49
3	57,84	37,71	20,13	1,86	1,89
4	79,03	71,30	7,73	1,12	1,39
5	67,1	59,19	7,91	0,96	1,21
6	103,84	99,02	4,82	0,94	0,82
7	100,39	99,15	1,24	0,24	0,68
8	71,66	67,38	4,28	0,66	0,87
9	67,39	60,16	7,23	1,19	1,78
10	82,06	74,09	7,97	1,20	0,79
average	79,37	72,44	6,92	0,94	1,04

Finally, the differences between the deceleration rates of the ten sites surveyed ($0,26 \text{ m/s}^2 \leq dm_{v85} \leq 1,25 \text{ m/s}^2$; $0,48 \text{ m/s}^2 \leq d85_{sv} \leq 1,37 \text{ m/s}^2$ along the distance L), suggest that the deceleration rate could be effected by other factors. Probably the variability of the deceleration rate among curves depends on the fact that the driver is affected by many factors resulting from the visual information of the curve ahead, such as curvature, pavement width, superelevation, sight distance available. Moreover, also the geometric characteristics of the upstream road alignment could affect the deceleration rate because they directly affect the approaching speed. In particular, the continuation of this research will focus on the relationships between the deceleration rate and the curve radius, as in the model used in the IHSDM (Fitzpatrick K. et al., 2000), and other factors as yet not analyzed such as the previous tangent length and the approaching speed. Meanwhile, while waiting for a regression analysis of the available data that might better explain those relationships, the deceleration rate proposed by Fitzpatrick for sharp radii was tested (Fitzpatrick K. et al.,

2000). This model assumes a constant deceleration rate of $1,00 \text{ m/s}^2$ for curves with radii lower than 175 m, even though the minimum curve radius of the sites where the speed data were collected to develop the model was 175 m. In this research, the average deceleration rates observed on sites with radii lower than 175 m (7 sites), are dm_{v85} $0,81 \text{ m/s}^2$ and $d85_{sv}$ $0,98 \text{ m/s}^2$ along the distance L , dm_{v85} $1,10 \text{ m/s}^2$ and $d85_{sv}$ $1,20 \text{ m/s}^2$ along the final 40 m before the point of curvature. Therefore, the rate adopted by the IHSDM model is more similar to the rate observed on the final part of the speed reduction, when the brake is applied, than to the average deceleration rate of all the speed reduction.

Finally, even though the analysis was limited to the tangents, the available data (sites 1, 4, 5, 7, 8, 10) confirmed that the deceleration continues along the curve after the point of curvature. However, the deceleration rate within the curve is lower than the average deceleration rate outside the curve.

CONCLUSION

Overall, the results suggest that a deceleration rate of $0,85 \text{ m/s}^2$ can be used in a simplified operating speed-profile even if this value represents only a rough approximation of the real deceleration rates that depend, in fact, on many factors. In effect, the results show that the deceleration rate varies along the distance travelled during speed reduction. In particular, the data show that in the final part of the speed reduction the deceleration rate is higher than in the first part. This difference leads to the conclusion that driver behaviour can be schematized in two phases: in the first the driver raises his foot from the accelerator and, in the second, he applies the brake. Moreover, the results show that the deceleration rate varies significantly between different sites. This difference could be due to many factors including the characteristics of the curve, of the upstream alignment, of the overall road environment. Therefore, additional data are recommended to estimate a deceleration model more accurately. The continuation of this research will investigate the difference of the deceleration rates between sites and along the distance travelled during speed reduction. Moreover, one of the two different approaches to calculate the deceleration rate from the speed data should certainly be chosen, according to the expected use.

Finally, the results show that single vehicles can reach deceleration rates much higher than the average deceleration rates observed, especially before curves with small radii. This fact should be considered both in the development of the deceleration model and in the definition of the safety improvements of sharp curves on existing roads.

REFERENCES

- Barjonet P., Lagarde D., Serveille J. (1992); *Sécurité Routière*; Presses de l'école Nationale des Ponts et Chaussées; Paris.
- Collins K.M., Krammes R.A. (1996); "Preliminary Validation of a Speed- Profile Model for Design Consistency Evaluation"; *Transportation Research Record*, No. 1523; Transportation Research Board; National Research Council; Washington D.C..
- Crisman B., Marchionna A., Perco P., Robba A., Roberti R. (2005); "Operating Speed Prediction Model for Two-Lane rural Roads"; *proceedings of the 3rd International Symposium on Highway Geometric Design*; Chicago, United States.
- Fitzpatrick K., Elefteriadou L., Harwood D., Collins J., McFadden J., Anderson I., Krammes R., Irizarry N., Parma K., Bauer K., Passetti K. (2000); *Speed Prediction for Two-Lane Rural Highways*; Report FHWA-RD-99-171; FHWA U.S. Department of Transportation.
- Hirsh M. (1987); "Probabilistic Approach to Consistency in Geometric Design"; *Journal of Transportation Engineering*, Vol. 113, n°3.
- Holmquist C. (1970); *Changes in Speeds of Vehicles on Horizontal Curves*; Report 104; National Road Research Institute; Sweden.
- Kockelke W., Steinbrecher J. (1987); *Driving Behaviour Investigations with Respect to Traffic Safety in the Area of Community Entrances*; Report of the Research Project 8363 of the German Federal Research Institute (Bundesanstalt für Strassenwesen Bereich Unfallforschung - BAST); n°153; Bergisch Gladbach, Germany.
- Krammes R.A., Brakett R. Q., Shaffer M. A., Ottesen J. L., Anderson I. B., Fink K. L., Collins K. M., Pendleton O. J., Messer C. J. (1995); *Horizontal Alignment Design Consistency for Two-Lane Highways*; Report FHWA-RD-94-034; FHWA, U.S. Department of Transportation.
- Lamm R., Choueiri E.M. (1987); "Recommendations for Evaluating Horizontal Design Consistency Based on Investigations in the State of New York"; *Transportation Research Record*, No. 1122; Transportation Research Board; National Research Council; Washington D.C..
- Lamm R., Choueiri E.M., Hayward J. C., (1988); "Tangent as an Independent Design Element"; *Transportation Research Record*, No. 1195; Transportation Research Board; National Research Council; Washington D.C..
- McFadden J., Elefteriadou L. (2000); "Evaluating Horizontal Alignment Design Consistency of Two-Lane Rural Highway: Development of New Procedure"; *Transportation Research Record*, No. 1737; Transportation Research Board; National Research Council; Washington D.C..

Ministry of Infrastructures and Transportation (2001); *Norme funzionali e geometriche per la costruzione delle strade*; D.M. 05/11/2001; Italy.

Perco P., Crisman B. (2004); "Influence of Spiral Length on Path of Vehicle entering a Curve"; *proceedings of the 83rd Transportation Research Board Annual Meeting*, Washington D.C..

Perco P. (2005); "Comparison between Vehicle Paths along Transition Sections with and without Spiral Curves"; *proceedings of the 3rd International Symposium on Highway Geometric Design*; Chicago, United States.

Steierwald, G., Buck M., 1992; *Speed Behaviour on Two-Lane rural Roads with regard to Design, Operational and Traffic Related Conditions*, Research Road Construction and Traffic Tecnique (Forschung Strassenbau und Strassenverkehrstechnik), vol. 621 Ministry of Transportation, Germany.

Swiss Association of Road Specialists (Vereinigung Schweizerischer Strassenfachleute VSS) (1981); Swiss Norm SN 640 080 a/b, Speed as a Design Element of the horizontal alignment; Zurich, Switzerland.

Taragin A. (1954); "Driver Performance on Horizontal Curve"; *Public Roads*, vol. 28 n°2.

ACKNOWLEDGMENTS

Thanks are due to the CSPA (Centro Servizi Polivalente di Ateneo) of the Università degli Studi di Trieste for having made it possible to use their Lidar gun

The authors wish to thank the road administration for their collaboration:

ANAS S.p.A. – Compartimento per la Viabilità del Friuli Venezia Giulia

Provincia di Trieste – Area I Viabilità

Provincia di Gorizia – Direzione N.4 - Viabilità e Trasporti